J Fusion Energ (2011) 30:39–47
DOI 10.1007/s10894-010-9338-3

ORIGINAL RESEARCH

Neon Soft X-Ray Yield Optimization from PF-SY1 Plasma Focus Device

M. Akel · Sh. Al-Hawat · S. Lee

Published online: 25 September 2010

Abstract Based on the consideration of that for operation of the plasma focus in neon, a focus pinch compression temperature of 200–500 eV (2.3×10^6–5×10^6 K) is suitable for good yield of neon soft X-rays (SXR), numerical experiments have been investigated on the plasma focus device PF-SY1 using the latest version Lee model code. The Lee model code is firstly applied to characterize the PF-SY1 Plasma Focus. Keeping the bank parameters and operational voltage unchanged but systematically changing other parameters, numerical experiments were performed finding the optimum Y_{sxr} was 0.026 J. Thus we expect to increase the neon Y_{sxr} of PF-SY1 from its present typical operation; without changing the capacitor bank and the electrode configuration merely by changing the operating pressure. The Lee model code was also used to run numerical experiments on PF-SY1 with neon gas for optimizing soft X-ray yield with reducing L_0, varying z_0 and 'a'. From these numerical experiments we expect to increase the neon Y_{sxr} of PF-SY1 with reducing L_0, from the present 0.026 J at $L_0 = 1600$ nH to maximum value of near 26 J at an achievable $L_0 = 10$ nH.

M. Akel (✉) · Sh. Al-Hawat
Department of Physics, Atomic Energy Commission, Damascus, P.O. Box 6091, Syria
e-mail: pscientific@aec.org.sy

S. Lee
Institute for Plasma Focus Studies, 32 Oakpark Drive, Chadstone, VIC 3148, Australia

S. Lee
National Institute of Education, Nanyang Technological University, Singapore 637616, Singapore

S. Lee
INTI International University College, 71800 Nilai, Malaysia

Keywords PF-SY1 Low energy plasma focus device · Soft X-ray · Neon gas · Lee model RADPF5.15K

Introduction

Plasma focus has been demonstrated as potential X-ray source for various medico-biological and industrial applications such as lithography (using ~0.9–1.5 keV photons) [1–4], radiography [5, 6], microscopy (using ~0.25–2.5 keV radiations) [7, 8], and micromachining (using ~4 keV photons) [9]. This has led to an increasing interest in exploiting the plasma focus device as a viable intense X-ray source due to some clear advantages such as being relatively cheap, compact, and ease of construction. The X-ray emissions from plasma focus devices have been explored over the wide range of capacitor bank energies ranging from large mega joule and few hundred kilo joule banks [10] to medium sized kilo joule banks [4, 11–14] to sub kilo joule banks of miniature sized focus devices [15–17]. In the last few years various efforts have been made for enhancing the X-ray yield by changing various experimental parameters such as bank energy [18], discharge current, electrode configuration (shape and material) [11, 13], insulator material and dimensions [11], gas composition and filling gas pressure [5]. Thus, soft X-ray yield optimization studies on the plasma focus devices operating over the wide range of bank energies have been one of the actively pursued fields of plasma focus research owing to their vast possible applications. Currently used systematic trial and error experimental procedure to obtain the optimized conditions for maximum radiation yield is highly time-consuming. Hence, the quicker optimization of plasma focus device is highly desirable which can be achieved if the reliable focus model and corresponding simulation code to predict the X-ray

yields from plasma focus device can be developed and used. Obviously the computed yields need to be checked against corresponding measured yields. Further, if the computed soft X-ray yields are consistently reliable against measured values, then it is reasonable to use the computed gross plasma properties as indicative of what we can expect when these plasma properties are measured. In this way, a reliable model code can not only be used to compute radiation yields, but also be used as a good indicative diagnostic tool for multiple gross plasma properties of the plasma focus [17].

Mahe [19] and Bing [20] reported that for operation in neon, a focus pinch compression temperature of 200–500 eV (2.3×10^6–5×10^6 K) is suitable for good yield of neon soft X-rays (SXR).

The Lee model code has been successfully used to perform numerical experiments to compute neon soft X-ray yield for the NX2 as a function of pressure with reasonable degree of agreement in (1) the Y_{sxr} versus pressure curve trends, (2) the absolute maximum yield and (3) the optimum pressure value. The only input required is a measured total current waveform. This reasonably good agreement, against the background of an extremely complicated situation to model, moreover the difficulties in measuring Y_{sxr}, gives confidence that the model is sufficiently realistic in describing the plasma focus dynamics and soft X-ray emission for NX2 operating in Neon [17].

Numerical experiments for the UNU/ICTP PFF capacitor system using the Lee model code have shown that even more drastic shortening of anode length z_0 is required, from the original 16 to 7 cm; at the same time increasing the anode radius 'a' from 0.95 to 1.2 cm, to obtain an optimum yield of $Y_{sxr} = 9.5$ J. This represents a 2- to 3-fold increase in Y_{sxr} from that computed for the standard UNU/ICTP PFF [21].

In this paper, we use the latest version of Lee Model RADPF5.15K for optimization of the PF-SY1 plasma focus device for neon soft X-ray operation.

The Model Code Used for Numerical Experiments

The dynamics of plasma focus discharges is complicated; for this purpose, to investigate the plasma focus phenomena, the Lee model couples the electrical circuit with plasma focus dynamics, thermodynamics and radiation, enabling realistic simulation of all gross focus properties.

In the radial phases, axial acceleration and ejection of mass are caused by necking curvatures of the pinching current sheath result in time-dependent strongly center-peaked density distributions. Moreover laboratory measurements show that rapid plasma/current disruptions result in localized regions of high densities and temperatures particularly in the heavy gases like xenon. We need to point out that these center-peaking density effects and localized regions are not modeled in the code, which consequently computes only an average uniform density and an average uniform temperature which are considerably lower than measured peak density and temperature. However, because the four-model parameters are obtained by fitting the computed total current waveform to the measured total current waveform, the model incorporates the energy and mass balances equivalent, at least in the gross sense, to all the processes which are not even specifically modeled. Hence the computed gross features such as speeds and trajectories and integrated soft X-ray yields have been extensively tested in numerical experiments for several machines and are found to be comparable with measured values.

Thus the code provides a useful tool to conduct scoping studies, as it is not purely a theoretical code, but offers means to conduct phenomenological scaling studies for any plasma focus device from low energy to high energy machines.

The model in its two-phase form was described in 1984 [22]. It was successfully used to assist in the design and interpretation of several experiments [23–26]. Radiation-coupled dynamics was included in the five-phase code leading to numerical experiments on radiation cooling [27]. The vital role of a finite small disturbance speed discussed by Potter in a Z-pinch situation [28] was incorporated together with real gas thermodynamics and radiation-yield terms. Before this 'communication delay effect' was incorporated, the model consistently over-estimated the radial speeds by a factor of ~ 2 and shock temperatures by a factor ~ 4. This version using the 'signal-delay slug' assisted other research projects [4, 20, 29] and was web-published in 2000 [30] and 2005 [31]. All subsequent versions of the Lee model code incorporate the 'signal-delay slug' as a must-have feature. Plasma self-absorption was included in 2007 [30] improving soft X-ray yield simulation in neon, argon and xenon among other gases. The model has been used extensively as a complementary facility in several machines, for example, UNU/ICTP PFF [4, 23, 25, 29, 32–35], NX1 [4, 36] NX2 [4, 20] and DENA [37]. It has also been used in other machines for design and interpretation including sub-kJ plasma focus machines [38]. Information obtained from the model includes axial and radial velocities and dynamics [37], dimensions and duration of the focus pinch, gross information of temperatures and densities within the pinch, soft X-ray emission characteristics and yield [4, 20, 39], design and optimization [38, 39], of machines, and adaptation to other machine types such as the Filippov-type DENA [37]. The versatility and utility of the improved model is demonstrated in the clear distinction of pinch current from the peak current [40]

and the recent uncovering of a plasma focus pinch current limitation effect [41–44]. The detailed description, theory, latest code and a broad range of results of this 'Universal Plasma Focus Laboratory Facility' are available for download from ref. [45].

X-Ray Emissions in Plasma Focus and Its Incorporation in Model Code

The focused plasma, with electron temperature of a few hundreds eV to about keV and high enough electron density, is a copious source of X-rays. The plasma focus emits both soft (thermal) as well as hard (non-thermal) X-rays but for the scope of this paper we will concentrate only on soft thermal X-rays. The plasma focus emits soft thermal X-rays by three processes [46, 47], namely: Bremsstrahlung (free–free transition) from the coulomb interactions between electrons and ions; recombination radiation (free–bound transition) emitted by an initially free electron as it loses energy on recombination with an ion; and de-excitation radiation (bound–bound transition) when a bound electron loses energy by falling to a lower ionic energy state. The first two processes give rise to the continuum of the X-ray spectrum while the third process produces the characteristic line radiation of the plasma. The relative strengths of the continuum and line emissions depend on how the plasma was formed; typically, for plasma formed from a high-Z material continuum emission dominates, while for a low-Z material line emission can be stronger. The calculation of the power emitted by processes within the plasma depends on assumptions made about the state of the plasma.

In the code [17, 21, 45, 48] in pinch phase, line radiation Q_L is calculated using the relation

$$\frac{dQ_L}{dt} = -4.6 \times 10^{-31} N_i^2 Z_{\text{eff}} Z_n^4 (\pi a_{\text{min}}^2) Z_{\text{max}}/T \qquad (1)$$

after being integrated over the pinch duration. Hence the soft X-ray energy generated within the plasma pinch depends on the properties: number density N_i, effective charge number Z_{eff}, atomic number of gas Z_n, pinch radius a_{min}, pinch length Z_{max}, plasma temperature T and the pinch duration. This generated energy is then reduced by the plasma self-absorption which depends primarily on density and temperature; the reduced quantity of energy is then emitted as the soft X-ray yield.

These effects are included in the modeling by computing volumetric plasma self-absorption factor 'A' derived from the photonic excitation number M which is a function of the Z_n, N_i, Z and T.

Based on the corona model, in the code we take the neon soft X-ray yield (generation H-like and He-like ions) to be equivalent to line radiation yield i.e., $Y_{\text{sxr}} = Q_L$ at the following temperature range 200–500 eV.

PF-SY1: The Numerical Experiments

The plasma focus PF-SY1 was described in ref. [49]. An Ohmic voltage divider 1:100 and a Rogowskii coil were used to determine the voltage and total current traces versus time during the plasma focus process, using a TDS storage oscilloscope with 1:10 attenuator.

The bank parameters were: $L_0 = 1430$ nH, $C_0 = 25$ μF and $r_0 = 50$ mΩ.
The tube parameters were: $b = 3.2$ cm, $a = 0.95$ cm, and $z_0 = 16$ cm.

The operating parameters were $V_0 = 15$ kV, and $p_0 = 0.675$ Torr, filling neon gas, where L_0 is the static inductance (nominal), C_0 the storage capacitance (nominal), b the outer radius, "a" the inner radius, z_0 the anode length, V_0 the operating voltage and p_0 the operating initial pressure. The measured current waveform at the above conditions is shown in Fig. 1. It can be noticed that the peak value of total discharge current I_{peak} is about 48 kA and focusing time occurs at about 10 μs.

We first digitize the measured current waveform using an open access source digitizing program, Engauge [50] and then we fit the computed current waveform to the measured waveform as follows:

We configure the Lee model code (version RADPF5.15K) to operate as the PF-SY1 plasma focus starting with the above bank and tube parameters.

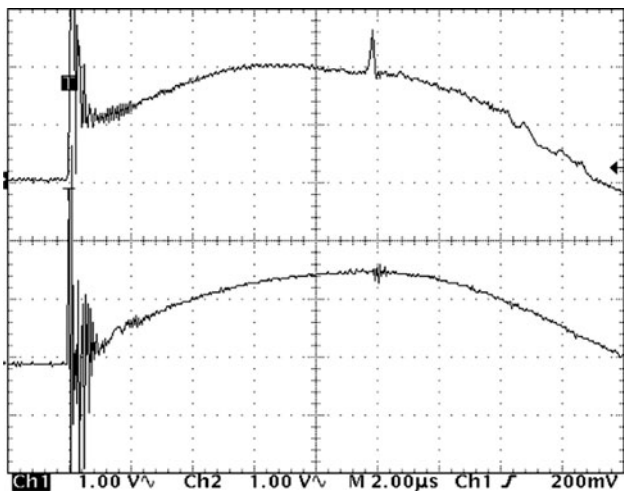

Fig. 1 The temporal evolution of voltage (*up*) and current (*down*) of the neon discharge during the plasma focus formation in PF-SY1, (1vert. div = 1 kV for voltage; and 32 kA for current). $p_0 = 0.675$ Torr, $C_0 = 25$ μF, $L_0 = 1430$ nH, $r_0 = 50$ mΩ, $V_0 = 15$ kV

To obtain a reasonably good fit the following parameters are used:

Bank parameters: $L_0 = 1600$ nH, $C_0 = 25$ μF, $r_0 = 77$ mΩ,
Tube parameters: b = 3.2 cm, $a = 0.95$ cm, $z_0 = 16$ cm,
Operating parameters: $V_0 = 15$ kV, $p_0 = 0.675$ Torr, neon gas,

together with the following fitted model parameters:

$f_m = 0.078, f_c = 0.7, f_{mr} = 0.15$ and $f_{cr} = 0.7$.

It can be seen that the computed discharge current waveform agrees well with the measured current waveform (Fig. 2).

The numerical experiments using RADPF5.15K at the bank and tube parameters last mentioned above and using the fitted model parameters give then the following results: the end axial speed to be $V_a = 2.6$ cm/μs, the speed factor is 60 kA/cm per [Torr of Neon]$^{1/2}$, the final plasma column is 0.06 cm in radius, and 1.3 cm in length (see Table 1).

Soft X-Ray Yield Versus Pressure

As the first step, the code RADPF5.15K was run to optimize X-ray yield from PF-SY1 with neon gas as function of only pressure; fixing all the mentioned above parameters. The pressure was varied from 0.08 to 2.7 Torr.

As it is well known, when the operating pressure is increased, the plasma speeds decrease; hence, the duration of the axial phase increases. From Table 1 it is seen that the Y_{sxr} increases with increasing pressure until it reaches the maximum value about 0.026 J at $p_0 = 0.37$ Torr, after which it decreases with higher pressures. As expected as p_0 is increased, the end axial speed, the inward shock speed and the radial piston speed all reduced. The decrease in speeds lead to lowering of plasma temperatures below that needed for soft X-ray production. Figure 3 presents the X-ray yield and temperature as functions of the pressure. From Table 1 we note that a shift of operating pressure to 0.37 Torr would increase the computed Y_{sxr} to 0.026 J at $V_a = 3.3$ cm/μs.

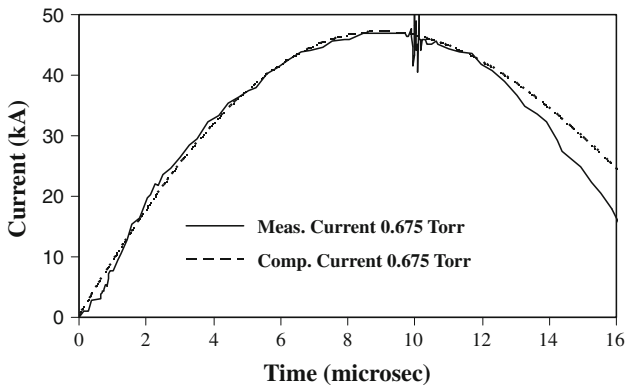

Fig. 2 Comparison of the computed current trace (*dotted line*) with the experimental one (*solid smooth line*) of the PF-SY1 at 15 kV, 0.675 Torr at neon filling gas

It is also evident from Table 1 that the peak value of total discharge current I_{peak} slightly decreases with decreasing pressure. This is due to increasing dynamic resistance (rate of change of plasma inductance, *dL/dt* gives rise to a dynamic resistance equal to 0.5 *dL/dt*) due to the increasing current sheath speed as pressure is decreased. We note that, on the contrary, the current I_{pinch} that flows through the pinched plasma column increases with decreasing pressure until reaches the maximum. This is due to the shifting of the pinch time closer and closer towards the time of peak current as the current sheet moves faster and faster [39]. As the pressure is decreased, the increase in I_{pinch} may be expected to favour Y_{sxr}; however, there is a competing effect that decreasing pressure reduces the number density. The interaction of these competing effects will decide on the actual yield versus pressure behavior as shown in the computed results. Figure 4 presents the total discharge current I_{peak} and the current I_{pinch} as functions of the pressure.

Soft X-Ray Yield Versus Pressure and Electrode Geometry

To optimize the soft X-ray yield from PF-SY1 Plasma focus with neon gas, more numerical experiments were carried out with the above model parameters; but varying p_0, z_0 and 'a' keeping $c = b/a$ constant at value $c = 3.368$. The pressure p_0 was varied from 0.6 to 6 Torr.

The following procedure was used [51, 52]:

- At each p_0, the anode length z_0 was fixed at a certain value,
- Then the anode radius 'a' was smoothly varied, till the maximum X-ray yield (Y_{sxr}) was obtained for this certain value of z_0.
- After that, we chose another value of z_0, varying the value of 'a' looking for the maximum of Y_{sxr}, until we found the optimum combination of z_0 and 'a' for the best X-ray yield at the fixed p_0.
- Then we changed p_0 and repeated the above procedure to find the optimum combination of z_0 and 'a' corresponding to this new value of p_0. We proceed until we had obtained the optimum combination of p_0, z_0 and 'a' for the maximum soft X-ray yield.

For optimum neon Y_{sxr}, as mentioned earlier, there is an optimum temperature. This implies that there is an optimum speed factor [27] $S = (I_{peak}/a)/p_0^{0.5}$. As p_0 was increased in order to maintain the optimum S, (I_{peak}/a) had

Table 1 Variation PF-SY1 parameters with pressure at: $L_0 = 1600$ nH, $C_0 = 25$ μF, $r_0 = 77$ mΩ, $V_0 = 15$ kV, RESF = 0.304, $c = b/a = 3.368$, $f_m = 0.078$, $f_c = 0.7$, $f_{mr} = 0.15$, $f_{cr} = 0.7$, neon gas

p_0 (Torr)	I_{peak} (kA)	I_{pinch} (kA)	V_a (cm/μs)	V_s (cm/μs)	V_p (cm/μs)	Pinch dur. (ns)	Y_{sxr} (J)
2.8	The code unable to run						
2.50	47.4	15.8	1.20	4.0	3.7	43.4	0.000
2.00	47.4	21.7	1.41	6.6	5.8	24.7	0.000
1.50	47.3	26.7	1.70	9.7	8.0	16.7	0.000
1.00	47.2	30.8	2.12	13.1	10.4	13.0	0.000
0.80	47.2	32.0	2.36	14.8	11.7	11.5	0.000
0.68	47.1	32.5	2.55	16.6	12.6	10.3	0.000
0.60	47.1	32.7	2.69	17.7	13.2	9.8	0.000
0.50	47.1	32.8	2.90	19.6	14.1	8.9	0.000
0.40	46.8	32.7	3.17	21.9	14.8	8.2	0.000
0.37	46.6	32.6	3.27	22.8	15.1	7.9	0.026
0.36	46.6	32.5	3.30	23.2	15.1	7.8	0.024
0.35	46.5	32.5	3.34	23.6	15.2	7.6	0.021
0.33	46.3	32.4	3.41	24.5	15.4	7.4	0.016
0.30	46.0	32.2	3.53	24.9	15.6	7.6	0.013
0.25	45.3	31.7	3.77	25.1	16.2	8.0	0.008
0.20	44.2	30.9	4.08	25.7	16.7	8.1	0.004
0.15	42.6	29.8	4.49	26.9	17.8	8.1	0.002
0.10	40.1	28.1	5.11	29.0	19.9	7.7	0.001
0.08	38.7	27.1	5.49	30.6	21.3	7.4	0.000

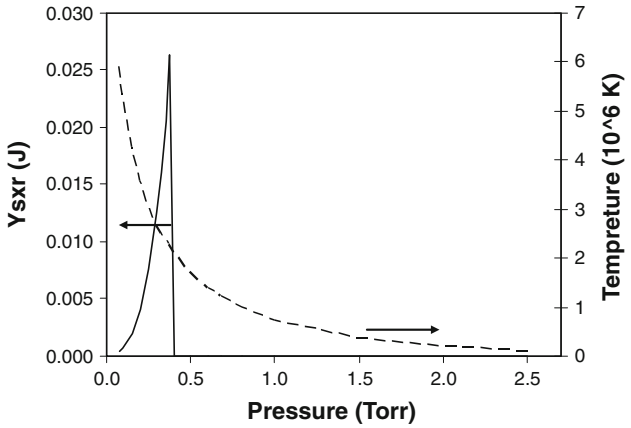

Fig. 3 The X-ray yield and temperature as functions of the pressure

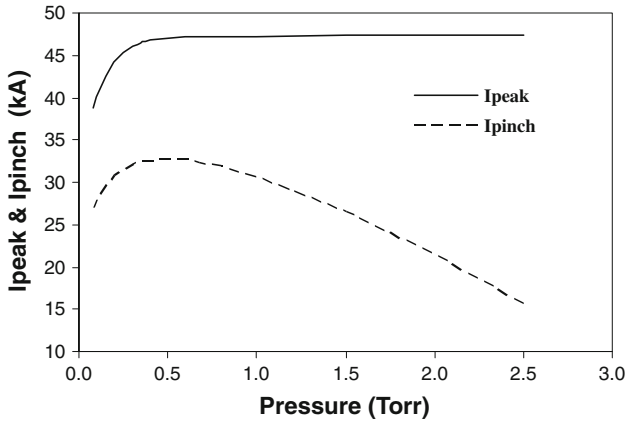

Fig. 4 Currents I_{peak} and I_{pinch} as functions of the pressure

to be correspondingly increased, by a reduction of 'a'. The numerical experiments also showed that z_0 needed to be increased to optimize the Y_{sxr} (see Table 2). Thus whilst external inductance L_0 is fixed at a constant value and an axial section inductance L_a is increased due to increasing the anode length, the pinch inductance L_p is reduced due to decreasing the pinch length [27, 43].

The optimized results for each value of p_0 are shown in Table 2. The table shows that as p_0 is increased, anode length z_0 rises and inner radius 'a' decreases with each increase in p_0, while the soft X-ray yield slightly increases with increasing p_0 until it reaches a maximum value of 0.026 J at $p_0 = 0.7$ Torr; then the Y_{sxr} decreases with further pressure increase.

Figure 5 shows X-ray yield as function of p_0, with the plasma focus operated at the optimum combination of z_0 and 'a' corresponding to each p_0. Figure 6 shows the corresponding optimum z_0 and 'a' as functions of pressure.

As p_0 was increased; the total current (I_{peak}) and the pinch current (I_{pinch}) slightly increased until they reached their maximum values, then slightly decreased with further increase in p_0 (see Fig. 7).

Table 2 X-ray yield optimization from PF-SY1 for each value of p_0 varying z_0 and 'a' at filling neon gas

p_0 (Torr)	z_0 (cm)	a (cm)	I_{peak} (kA)	I_{pinch} (kA)	Y_{sxr} (J)	V_a (cm/μs)	a_{min} (cm)	z_{max} (cm)
0.68	14.0	0.6900	45.7	32	0.023	3.20	0.06	0.93
0.70	19.0	0.6940	47.0	33	0.026	3.37	0.06	0.93
1.00	19.5	0.5810	47.0	33	0.025	3.36	0.05	0.78
1.50	20.0	0.4730	47.0	33	0.023	3.40	0.04	0.63
2.00	21.0	0.4090	47.0	33	0.023	3.43	0.04	0.55
2.50	21.5	0.3643	47.0	33	0.022	3.45	0.03	0.49
3.00	22.0	0.3320	47.0	32	0.021	3.46	0.03	0.44
3.50	23.0	0.3050	47.0	32	0.020	3.50	0.03	0.41
4.00	23.2	0.2853	47.0	32	0.020	3.50	0.02	0.38
4.50	23.5	0.2674	47.0	32	0.019	3.52	0.02	0.36
5.00	23.8	0.2540	47.0	32	0.018	3.52	0.02	0.34
5.50	24.0	0.2420	47.0	32	0.018	3.53	0.02	0.32

$L_0 = 1600$ nH, $C_0 = 25$ μF, $r_0 = 77$ mΩ, $V_0 = 15$ kV, RESF = 0.304, $c = b/a = 3.368$, $f_m = 0.078$, $f_c = 0.7$, $f_{mr} = 0.15$, $f_{cr} = 0.7$

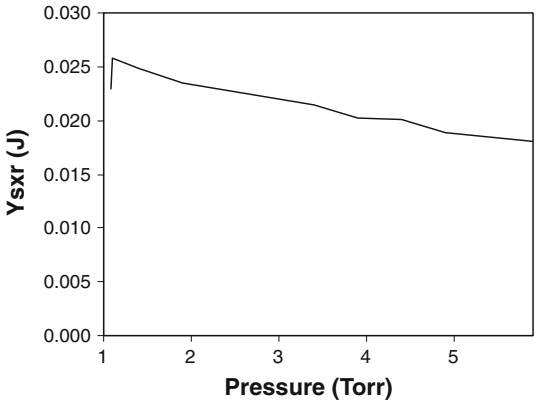

Fig. 5 The X-ray yield as function of pressure, anode length and inner radius (Y_{sxr} vs. p_0, z_0 and 'a')

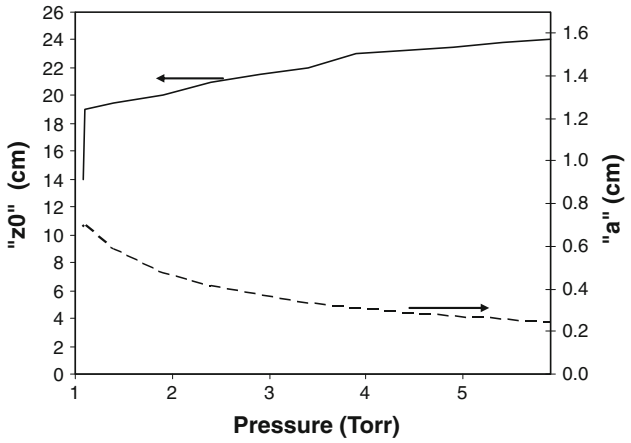

Fig. 6 Variation of the anode length and inner radius as functions of pressure

From the numerical experiments for PF-SY1 with $L_0 = 1600$ nH, $C_0 = 25$ μF, $r_0 = 77$ mΩ, $V_0 = 15$ kV we have thus found the optimum combination of p_0, z_0 and 'a' for neon Y_{sxr} as 0.7 Torr, 19 cm and 0.694 cm respectively.

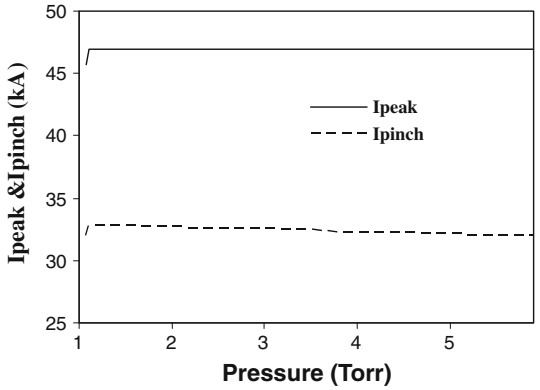

Fig. 7 Effect on currents I_{peak} and I_{pinch} as p_0 is increased from 0.68 to 5.5 Torr

This combination gives $Y_{sxr} = 0.026$ J. We also note that at this optimum configuration $I_{peak} = 47$ kA, $I_{pinch} = 33$ kA, and the end axial speed is of 3.4 cm/μs. The low optimum yield is due to the low I_{pinch} unavoidable because of the large value of L_0.

Nevertheless the numerical experiments have shown that with the present capacitor bank, PF-SY1 Plasma focus has a maximum Y_{sxr} at about 0.026 J.

We next note that practically it is technically difficult to change the dimensions of outer radius b; unless the whole electrode system and input flange system of the device is completely redesigned. On the other hand, if we keep the outer electrode unchanged and use a screw-on anode, the screw-on part can be designed to be screwed onto an anode stub that keeps the original radius until it just emerges out of the insulator sleeve, at which point it is cut short and has its radius converted to that of the screw-on part. Then the screw-on part of the anode can have the optimized radius 'a' and anode length z_0. The length of the cathode can be correspondingly shortened [21].

We therefore continue with the numerical experiments, keeping b = constant at the original value of 3.2 cm;

changing 'a' to 0.7 cm with $z_0 = 19$ cm; and varying pressure to find this 'practical optimum'. The results are shown in Table 3.

This gives us a practical optimum configuration of b = 3.2 cm (unchanged from the original cathode radius of the standard PF-SY1), $a = 0.7$ cm, $z_0 = 19$ cm, giving a practical optimum yield of 0.023 J at a p_0 of 0.66 Torr. The slightly lower yield compared with that in Table 2 is due to the increased ratio "c" from 3.4 to 4.6. An earlier study has shown that reducing c, down to certain limits, has a beneficial effect in the case of neutron production operating in deuterium, and we have also confirmed through numerical experiments that this effect is also observed for neon Y_{sxr}.

Soft X-Ray Yield Versus Inductance and Electrode Geometry

To optimize the soft X-ray yield from PF-SY1 with neon gas, varying L_0, z_0 and 'a' keeping 'c' and RESF constant. The external inductance L_0 was varied from 1600 to 1 nH.

The following procedures were used [44]:

At each L_0, the pressure was fixed at constant value (in our case $p_0 = 10$ Torr) and also the anode length was fixed at a certain value:

- Then the inner radius 'a' was varied, whilst keeping $c = 3.368$, until the maximum X-ray yield was obtained for this certain value of z_0.
- After that we chose another value of z_0, varying 'a' until maximum X-ray yield and so on, until we have obtained the combination of z_0 and 'a' for the best maximum X-ray yield at a fixed L_0 (Y_{sxr} vs. z_0 and 'a' at fixed L_0 and p_0).
- We repeated the above procedure for progressively smaller L_0 until $L_0 = 1$ nH.

The influence of L_0 reduction on the total current traces using RADPF5.15K was investigated. For example it was found that reducing L_0 increases the total current from $I_{peak} = 82$ kA at $L_0 = 500$ nH to $I_{peak} = 332$ kA at $L_0 = 25$ nH (see Table 4). As L_0 was reduced, I_{peak} increased; 'a' is necessarily increased leading to longer pinch length (Z_{max}), hence a bigger pinch inductance L_p. At the same time because of the reducing current drive time, z_0 needed to be reduced. The geometry moved from a long thin Mather-type to a shorter fatter one (see Table 4). Thus whilst L_0 and axial section inductance L_a reduced, the pinch inductance L_p increased due to increased pinch length.

At each L_0, after z_0 was varied, the inner radius 'a' was adjusted to obtain the optimum X-ray yield, which corresponds closely to the largest I_{pinch}.

The soft X-ray optimization for each value of L_0, varying z_0 and 'a' is shown in Table 4. The table shows that as L_0 is reduced, I_{peak} increases with each reduction in L_0 with no sign of any limitation as function of L_0. However, I_{pinch} reaches a maximum of 239.4 kA at $L_0 = 3$ nH, then it decreases with each reduction in L_0. Thus I_{peak} doesn't show any limitation as L_0 is progressively reduced. However, I_{pinch} has a maximum value. This pinch current limitation effect is not a simple, but it is a combination of the two complex effects: the interplay of the various inductances involved in the plasma focus processes abetted by the increasing coupling of C_0 to the inductive energetic processes, L_0 is reduced.

From Table 4 it can be seen, that as L_0 decreased, the soft X-ray yield increases until it reaches a maximum value

Table 3 Variation PF-SY1 parameters with pressure at: $L_0 = 1600$ nH, $C_0 = 25$ μF, $r_0 = 77$ mΩ, $V_0 = 15$ kV, RESF = 0.304, $c = b/a = 3.3507$, $b = 3.2$, $a = 0.955$, $z_0 = 13.4$, $f_m = 0.078$, $f_c = 0.7$, $f_{mr} = 0.15$, $f_{cr} = 0.7$, neon gas

p_0 (Torr)	I_{peak} (kA)	I_{pinch} (kA)	V_a (cm/μs)	V_s (cm/μs)	V_p (cm/μs)	Pinch dur. (ns)	Y_{sxr} (J)
1.9	The code unable to run						
2.20	47.3	16.1	1.4	6.3	5.6	19.0	0.000
2.00	47.2	18.7	1.5	8.1	6.9	14.7	0.000
1.80	47.2	21.1	1.6	9.6	8.0	12.3	0.000
1.40	47.2	25.7	1.9	12.7	10.2	9.9	0.000
1.00	47.1	29.6	2.3	16.9	12.8	7.5	0.000
0.80	47.0	31.2	2.6	20.0	14.3	6.5	0.000
0.70	47.0	31.8	2.8	22.0	14.9	6.0	0.000
0.68	47.0	31.9	2.8	22.7	15.0	5.8	0.000
0.67	46.9	32.0	2.8	22.9	15.0	5.8	0.000
0.66	46.9	32.0	2.8	22.8	15.1	5.8	0.023
0.66	46.9	32.0	2.8	23.0	15.1	5.7	0.022
0.63	46.9	32.2	2.9	24.2	15.3	5.4	0.017
0.60	46.9	32.3	3.0	24.8	15.5	5.5	0.014
0.50	46.8	32.6	3.2	25.1	16.2	5.8	0.009
0.40	46.7	32.6	3.5	25.9	16.9	5.9	0.004

Table 4 For each L_0 the optimization combination of z_0 and 'a' were found and are listed here

L_0 (nH)	z_0 (cm)	a (cm)	b (cm)	I_{peak} (kA)	I_{pinch} (kA)	a_{min} (cm)	Z_{max} (cm)	Y_{sxr} (J)
500	9.00	0.320	1.1	82	57.6	0.03	0.4	0.17
200	6.00	0.500	1.7	129	89.4	0.04	0.7	0.95
100	5.00	0.670	2.3	179	121.5	0.05	0.9	2.72
50	4.00	0.860	2.9	246	158.4	0.06	1.2	6.68
25	2.80	1.050	3.5	332	197.9	0.08	1.5	14.65
15	2.70	1.140	3.8	404	217.6	0.10	1.6	21.43
10	2.50	1.170	3.9	464	230.3	0.11	1.7	25.78
8	2.40	1.185	4.0	497	235.0	0.12	1.7	26.85
5	2.35	1.192	4.0	563	239.0	0.13	1.8	25.74
3	2.33	1.170	3.9	623	239.4	0.15	1.7	22.12
1	2.30	1.127	3.8	718	232.8	0.16	1.7	17.46

Bank parameters: $L_0 = 1600$ nH, $C_0 = 25$ μF, $r_0 = 77$ mΩ; tube parameter: $c = b/a = 3.368$; model parameters: $f_m = 0.078$, $f_c = 0.7$, $f_{mr} = 0.15$, $f_{cr} = 0.7$; operating at 10 Torr neon gas, $V_0 = 15$ kV

of 27 J at $L_0 = 8$ nH; beyond which the soft X-ray yield does not increase with reducing L_0. Thus with decreasing L_0 the pinch current I_{pinch} and the soft X-ray yield show limitation. The obtained results confirm the pinch current limitation effect in neon plasma focus, and consequently the soft X-ray yield. Figure 8 represents I_{pinch} and X-ray limitation effects in neon plasma focus at 10 Torr as L_0 is reduced from 500 to 1 nH.

Looking at Table 4, it is noticed that as L_0 was progressively reduced, to optimize 'a' had to be progressively increased and z_0 progressively decreased. Also the plasma pinch dimensions (pinch radius a_{min} and pinch length Z_{max}) increased as L_0 was reduced.

Based on the obtained results of these sets of numerical experiments on PF-SY1 with neon gas, we can say that to improve the soft X-ray yield, L_0 should be reduced to a value around 10–25 nH (which is an achievable range incorporating low inductance technology, below which the pinch current I_{pinch} and the soft X-ray yield Y_{sxr} would not be improved much, if at all. These experiments confirm the pinch current limitation effect, and consequently the soft X-ray yield for the neon plasma focus. Finally, we would like to emphasize that we, practically, have no intention (or ambition) to go below 10–15 nH (which is an achievable range), but in our numerical experiments using RADPF5.15K we go down to a low values of L_0 (8–1 nH) just to find the pinch current limitation effect.

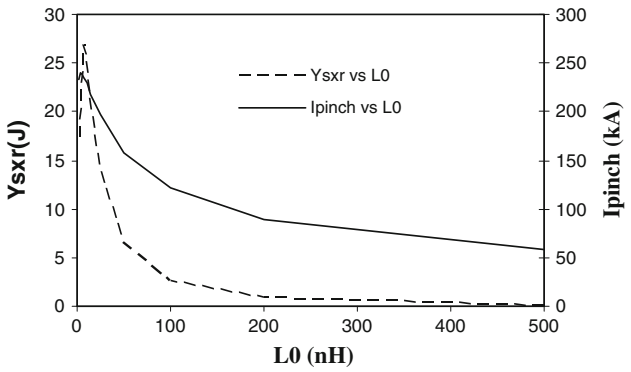

Fig. 8 The X-ray yield and I_{pinch} (computed) versus L_0 (500–1 nH)

Conclusions

The Lee model code was applied to characterize the PF-SY1 Plasma Focus, finding a maximium neon soft X-ray yield (Y_{sxr}) of 0.026 J, merely by changing the operating pressure.

The Lee model code was also used to run numerical experiments on PF-SY1 with neon gas for optimizing soft X-ray yield with reducing L_0, varying z_0 and 'a'.

Contrary to the general expectation that performance of a plasma focus would progressively improve with progressive reduction of its external inductance L_0, the pinch current limitation effect in plasma focus was confirmed with reducing L_0 (maximum I_{pinch} is about 239.4 kA at $L_0 = 3$ nH), and consequently the maximum soft X-ray yield was computed as 26.85 J at $L_0 = 8$ nH; operating the inductance-reduced PF-SY1 at 15 kV, 10 Torr neon pressure.

From these numerical experiments we expect to increase the neon Y_{sxr} of PF-SY1 with reducing L_0, from the present 0.026 J at $L_0 = 1600$ nH to maximum value of near 26 J at an achievable $L_0 = 10$ nH. Because of the current limitation effect, there is little to gain to try to reduce L_0 to 5 nH (which is technically very difficult); and even a loss to reduce L_0 below 5 nH.

Acknowledgments The authors would like to thank Director General of AECS, for encouragement and permanent support. M. Akel would also like to express thanks to Mrs. Sheren Isamael, who collaborated going through all the numerical experiments using Lee Model.

References

1. D. Wong, A. Patran, T.L. Tan, R.S. Rawat, P. Lee, IEEE Trans. Plasma Sci. **32**, 2227 (2004)

2. R. Petr, A. Bykanov, J. Freshman, D. Reilly, J. Mangano, M. Roche, J. Dickenson, M. Burte, J. Heaton, Rev. Sci. Instrum. **75**, 2551 (2004)
3. Y. Kato, I. Ochiai, Y. Watanabe, S. Murayama, J. Vac. Sci. Technol. B **6**, 195 (1988)
4. S. Lee, P. Lee, G. Zhang, X. Feng, V.A. Gribkov, L. Mahe, A. Serban, T.K.S. Wong, IEEE Trans. Plasma Sci. **26**, 1119 (1998)
5. F.N. Beg, I. Ross, A. Lorena, J.F. Worley, A.E. Dangor, M.G. Hanies, J. Appl. Phys. **88**, 3225 (2000)
6. S. Hussain, M. Shafiq, R. Ahmad, A. Waheed, M. Zakaullah, Plasma Sources Sci. Technol. **14**, 61 (2005)
7. F. Castillo-Mejia, M.M. Milanese, R.L. Moroso, J.O. Pouzo, M.A. Santiago, IEEE Trans. Plasma Sci. **29**, 921 (2001)
8. R.S. Rawat, T. Zhang, G.J. Lim, W.H. Tan, S.J. Ng, A. Patran, S.M. Hassan, S.V. Springham, T.L. Tan, M. Zakaullah, S. Lee, P. Lee, J. Fusion Energ. **23**, 49 (2004)
9. V.A. Gribkov, A. Srivastava, P.L.C. Keat, V. Kudryashov, S. Lee, IEEE Trans. Plasma Sci. **30**, 1331 (2002)
10. V.A. Gribkov, B. Bienkowska, M. Borowiecki, A.V. Dubrovsky, I. Ivanova-Stanik, L. Karpinski, R.A. Miklaszewski, M. Paduch, M. Scholz, K. Tomaszewski, J. Phys. D Appl. Phys. **40**, 1977 (2007)
11. M. Zakullah, K. Alamgir, M. Shafiq, S.M. Hassan, M. Sharif, S. Hussain, A. Waheed, Plasma Sources Sci. Technol. **11**, 377 (2002)
12. R.S. Rawat, T. Zhang, C.B.L. Phua, J.X.Y. Then, K.A. Chandra, X. Lin, A. Patran, P. Lee, Plasma Sources Sci. Technol. **13**, 569 (2004)
13. H. Bhuyan, S.R. Mohanty, N.K. Neog, S. Bujarbarua, R.K. Rout, J. Appl. Phys. **95**, 2975 (2004)
14. S. Lee et al., Am. J. Phys. **56**, 62 (1988)
15. R. Verma, P. Lee, S.V. Springham, T.L. Tan, M. Krishnan, R.S. Rawat, Appl. Phys. Lett. **92**, 011506 (2008)
16. P. Silva, J. Moreno, C. Pavez, L. Soto, J. Arancibia, J. Phys. Conf. Ser. **134**, 012044 (2008)
17. S. Lee et al., Plasma Phys. Control. Fusion **51**, 105013 (2009)
18. P.G. Burkhalter, G. Mehlman, D.A. Newman, M. Krishnan, R.R. Prasad, Rev. Sci. Instrum. **63**, 5052 (1992)
19. M.H. Liu, Soft X-ray from compact plasma focus. PhD Thesis, School of Science, Nanyang Technological University, December 1996
20. S. Bing, Plasma dynamics and X-ray emission of the plasma focus. PhD Thesis NIE ICTP Open Access Archive: http://eprints.ictp.it/99/, 2000
21. S.H. Saw, et al., IEEE Trans. Plasma Sci. **37**(7), 1276–1282 (2009)
22. S. Lee, in *Radiations in Plasmas,* ed. by B. McNamara (World Scientific, Singapore, 1984), pp. 978–987
23. T.Y. Tou, S. Lee, K.H. Kwek, IEEE Trans. Plasma Sci. **17**, 311 (1989)
24. S. Lee, IEEE Trans. Plasma Sci. **19**, 912 (1991)
25. A. Serban, S. Lee, J Plasma Phys. **60**, 3–15 (1998)
26. S. Lee, A. Serban, IEEE Trans. Plasma Sci. **24**, 1101–1105 (1996)
27. J.B. Ali, Development and studies of a small plasma focus. PhD thesis, University Technology Malaysia, Kuala Lumpur, Malaysia, 1990
28. D.E. Potter, Nucl. Fusion **18**(6), 813–823 (1978)
29. M.H. Liu et al., IEEE Trans. Plasma Sci. **26**, 135–140 (1998)
30. S. Lee, http://ckplee.myplace.nie.edu.sg/plasmaphysics/, 2000–2009
31. S. Lee, ICTP Open Access Archive: http://eprints.ictp.it/85/13, 2005
32. S. Lee, Twelve Years of UNU/ICTP PFF—A Review IC, 98, (231) ICTP, Miramare, Trieste; ICTP OAA: http://eprints.ictp.it/31/, 1998
33. S.V. Springham et al., Plasma Phys. Control. Fusion **42**, 1023–1032 (2000)
34. A. Patran et al., Plasma Sources Sci. Technol. **14**(3), 549–560 (2005)
35. M.A. Mohammadi, S. Sobhanian, C.S. Wong, S. Lee, P. Lee, R.S. Rawat, J. Phys. D. Appl. Phys. **42**, 045203 (2009)
36. E.P. Bogolyubov, et al., Phys. Scripta **57**, 488–494 1998
37. V. Siahpoush et al., Plasma Phys. Control. Fusion **47**, 1065 (2005)
38. L. Soto et al., Braz. J. Phys. **34**, 1814 (2004)
39. D. Wong et al., Plasma Sources Sci. Technol. **16**, 116–123 (2007)
40. S. Lee et al., Appl. Phys. Lett. **92**, 111501 (2008)
41. S. Lee et al., Appl. Phys. Lett. **92**, 021503 (2008)
42. S. Lee et al., Plasma Phys. Control. Fusion **50**, 065012 (2008)
43. S. Lee, S.H. Saw, Appl. Phys. Lett. **94**, 076102 (2009)
44. M. Akel, Sh. Al-Hawat, S. Lee, J. Fusion Energ. **29**, 1 (2010)
45. S. Lee, Radiative dense plasma focus computation package: RADPF (2009), http://www.intimal.edu.my/school/fas/UFLF/. http://www.plasmafocus.net/IPFS/modelpackage/File1RADPF.htm
46. E.H. Beckner, J. Appl. Phys. **37**, 4944 (1966)
47. W.H. Bostic, V. Nardi, W. Prior, J. Plasma Phys. **8**, 1 (1972)
48. Sh. Al-Hawat, S. Saloum, Contrib. Plasma Phys. **49**(1-2), 5–14 (2009)
49. S. Al-Hawat, IEEE Trans. Plasma Sci. 32(2), 764–769 (2004)
50. http://sourceforge.net/project/showfiles.php?group id = 67696&package id = 130007&release id = 500277, 2009
51. M. Akel, Sh. Al-Hawat, S. Lee, J. Fusion Energ. **28**(4), 355–363 (2009)
52. M. Akel, Sh. Al-Hawat, S.H. Saw, S. Lee, J. Fusion Energ. **29**, 223–231 (2010)